



OPEN

Different Zn loading in Urea–Formaldehyde influences the N controlled release by structure modification

Amanda S. Giroto¹, Stella F. do Valle^{1,2}, Gelton G. F. Guimarães³, Nicolai D. Jablonowski⁴✉, Caue Ribeiro¹✉ & Luiz Henrique C. Mattoso¹

Nitrogen fertilization has been a critical factor for high crop productivity, where urea is currently the most used N source due to its high concentration and affordability. Nevertheless, urea fast solubilization leads to frequent losses and lower agronomic efficiency. The modification of urea structure by condensation with formaldehyde has been proposed to improve nutrient uptake by plants and to reduce environmental losses. Herein we show that the co-formulation with Zn strongly modifies the N release (in lab conditions) and, more important, the Zn source—ZnSO₄ or ZnO—has a critical role. Urea–formaldehyde (UF) served as a matrix for the zinc sources, and chemical characterizations revealed that Zn particles influenced the length of the polymeric chain formation. Release tests in an aqueous medium showed that the UF matrix favors ZnO release and, on the other hand, delays ZnSO₄ delivery. Soil incubation with the fertilizer composites proved the slow-release of N from UF, is ideal for optimizing nutritional efficiency. Our results indicated that the ZnO-UF system has beneficial effects for both nutrients, i.e., reduces N volatilization and increases Zn release.

Boosts in modern agriculture are crucial to manage the increasing demand for food and other agro-products with the current trend of world population rapid growth. Chemical fertilizers have been essential to increase global agricultural production by approximately 50% over the last decades^{1,2}. Most technological advances are related to N-based fertilizers, especially urea, the most commonly used N-fertilizer worldwide. Due to its high N content and safe handling, it is the least expensive fertilizer in terms of transportation cost per unit of nutrient and affordable to most farmers^{3,4}. Unfortunately, its high water solubility leads to N losses, especially by volatilization, exceeding 50% of the total N applied and resulting in low fertilizer use efficiency^{1,2,5,6}.

In this context, slow-release fertilizers (SRFs) have been shown as a promising approach to manage losses and improve nutrient use efficiency². Urea–formaldehyde (UF) is one of the most common and the first group of products developed for SRFs fertilizer^{7–11}. UF fertilizers are based on condensation products, mainly comprised of urea–formaldehyde polymers with different polymerization degrees¹². UF is hydrolyzed by microorganisms in soil into ammonium, carbon dioxide, and water, allowing N absorption by plants. It also leads to complete compound degradation, i.e., an environmentally-friendly approach¹³. Besides all the positive points of UF fertilizers, their global market and production have been falling. Researchers argue that UF macromolecules' structure and crystallinity interfere in the material's short term biodegradation, being the main reason for the fertilizer industry to avoid this kind of product. The UF preparation can be modified using different processes to manage this aspect, e.g., solid-state processing, which abstains the use of extra reagents⁸; use of lower molar ratio between formaldehyde and urea producing shorter polymer chains and also urea units at the end of the chain; and reduction of hydrogen bond formation between UF chains to reduce crystallinity, thus improving the slow-release property¹⁴. The addition of some particles in the UF fertilizers during processing can reduce crystallinity by disturbing the regular UF molecular arrangement. In this sense, the introduction of a micronutrient source into the UF materials is beneficial. Some studies have indicated that the combined application of Zinc (Zn) and

¹National Nanotechnology Laboratory for Agribusiness (LNNA), Embrapa Instrumentação, XV Novembro Street, CP: 741, São Carlos, SP 13560-206, Brazil. ²Department of Chemistry, Federal University of São Carlos, Washington Luiz Highway, km 235, São Carlos, SP 13565-905, Brazil. ³Agricultural Research and Rural Extension Company of Santa Catarina, 6800 Highway, Antônio Heil, Itajaí, Santa Catarina 88318112, Brazil. ⁴Forschungszentrum Jülich GmbH, Institute of Bio- and Geosciences, IBG-2: Plant Science, 52425 Jülich, Germany. ✉email: n.d.jablonowski@fz-juelich.de; caue.ribeiro@embrapa.br

N fertilizers, for instance, promotes better nutrient absorption in crops for both elements. We propose that the micronutrient should be incorporated in the macronutrient fertilizer structure, as many fertilizer industries have been trying to do^{15–17}.

Nevertheless, as much as crops require Zn in small quantities, the element is necessary for plant growth and survival as an essential constituent of many enzymes and proteins. Zinc deficiency is especially concerning in places with high cereal consumption in diets, reflecting directly in human nutritional health problems^{4,18}. Zn is available for fertilization as zinc sulfate (ZnSO_4), zinc carbonate (ZnCO_3), zinc nitrate [$\text{Zn}(\text{NO}_3)_2$], zinc chloride (ZnCl_2), and zinc oxide (ZnO)¹⁹. ZnO has the highest Zn content, i.e., 80% Zn/ZnO (w/w), making it the most cost-effective, although zinc sulfate is more often used due to its high solubility^{20,21}.

Thus, herein we demonstrate that the Zn loading in UF structure affects N and Zn release in different forms depending on the Zn source. We have prepared slow-release fertilizers from UF with the addition of two sources of Zn (ZnO and ZnSO_4), using the melting mix process strategy. This process is environmentally-friendly, easy to operate, and suitable for industrial production. The effects of the Zn sources in particle loading were thoroughly investigated using FTIR-ATR, TG/DTG, and ^1H -, ^{13}C -NMR, to verify changes in the morphology and structure that could influence their nutrient release profile. The dynamics of both N and Zn were investigated by release in water medium tests, and a release test of N in soil. In addition, a poor soil (with low N holding capacity and high Zn leaching capacity) was chosen to monitor the volatilization losses in lab conditions.

Results and discussions

Scanning electron microscopy (SEM) shows that urea is composed by agglomerated particles higher than 200 μm (Fig. 1a). The reaction with paraformaldehyde (UF) resulted in a heterogeneous morphology (Fig. 1b), with uneven surfaces covered by needle-shaped crystals, corresponding to the urea–formaldehyde fraction^{22,23}. A new morphology is seen for the composites UFZO 0.5, 1, and 2 (Fig. 1e–g). ZnO probably acted as a catalyst in urea polycondensation, changing the polymeric structure to rectangular crystals (5–50 μm). These should not be ascribed as pure zinc oxide (Fig. 1c) or pure UF polymer due to the morphology differences. It indicates that the polymer is being nucleated by ZnO particles' surface, as seen by the good dispersion in EDX (Fig. S1, Supplementary Information). In contrast, the composites UFZS 0.5, 1, and 2, (Fig. 1h–j) present needle-shaped crystal formation, closer to pure UF, but with a superior size (superior to 50 μm), which is associated also to the dispersion of the ZnSO_4 particles over the polymer (Fig. S1, Supplementary Information). Possibly, ZnSO_4 is partly solubilized during processing, by the water that is released during the reaction of urea and formaldehyde. After solubilization, zinc sulfate presents a higher dispersion throughout the polymer, and precipitates as needles during the drying process. Therefore, ZnSO_4 has acted as an electrostatic dispersing agent instead of a particle where the polymer is being nucleated.

The typical FTIR spectra of ZnO, ZnSO_4 , UF, UFZO, and UFZS are shown in Fig. 2, Fig. S2 (inset) and Table S1 (peak assignment). The identification of free NH_2 groups shows that all composites have a polymer structure like urea:urea–formaldehyde as observed by Giroto et al.⁸. Thus, the materials have a mixed structure attributed to mono- or di-(hydroxymethyl) ureas, unreacted urea and linear polymerized urea chains. The region from 3350 to 3450 cm^{-1} is related to hydrogen-bonded O–H and N–H, mainly attributed to monomers such as water and formaldehyde, whose O–H group may form H bonds with reactive functional groups such as CH_2OH , NH_2 , and N–H²⁴. A major broad peak is seen for UFZO 2 (Fig. 2a) compared to the others. No residual paraformaldehyde was detected in the polymers²⁵. Other characteristic peaks are amide I, II, and C=O, which were shifted to lower frequencies for both pure UF and all composites. The dislocation strongly indicates a partial hydrogen-bond (H-bond) formation between C=O and N–H groups when the urea–formaldehyde polymer is formed. It is possible that the samples have partial hydrogen bonds due to the C=O bond with or without H-bonds. A high concentration of methylene-bridge bonds (N– CH_2 –N) was detected²⁶. These bands, together with the strong bands of C–N, C–O stretching in hydroxymethyl urea, and methylene ether linkage C–O–C, prove the formation of the structure of multiple methyl urea in the polymeric chain^{14,27,28}. UFZO 2 was the only material to differ from the others, especially at 1700–1445 cm^{-1} , very likely due to a higher H-bond formation between the multiple hydroxyethyl urea chains with different size lengths.

XRD patterns were conducted to study the crystalline structures of the samples. As shown in Fig. 3a, the existence of crystalline regions in UF is confirmed, possibly belonging to hydroxymethyl urea crystallized by H bonding during aging^{29–31}. Peaks of ZnO were identified in the composites and no modification in UF pattern was seen, which indicates that the load did not change the UF crystalline phase. The same crystallization behavior was observed in Fig. 3b for UFZS composites. However, no signal of crystalline ZnSO_4 particles was detected. In this case, the water released during urea polycondensation with formaldehyde might have solubilized embedded ZnSO_4 . In both composites, an increase on polymer signals is verified according to the Zn ratio. A broad peak in the range $2\theta=10$ – 30° , attributed to the amorphous region in UFZO 1, UFZO 2, UFZS 0.5, UFZS 1 and UFZS 2, suggests ramification or cross-linking during the condensation. Analysis of the amplified area at 21 – 23° (Fig. 3c,d) indicates the breakdown of the urea crystallinity of the composites UFZO 1, UFZO 2, UFZS 0.5, UFZS 1, and UFZS 2. It evidences the interactions of ZnO and ZnSO_4 with UF. For UF, peaks at 22.2° and 22.4° of urea shifted to 21.9° and 22.2° , respectively, very likely due to the hydroxyethyl urea chains. UFZO 0.5 was the only one to maintain a crystalline peak of pure urea at 22.4° .

The urea–paraformaldehyde reaction was investigated by thermoanalytical methods. Figure 4 shows the DSC thermograms for UF materials. The endothermic event of urea melting (135 $^\circ\text{C}$) shifted to lower temperatures (from 115 to 122 $^\circ\text{C}$) in reacted materials, indicating the melting of oligomeric fractions or decomposition of bridges³². This peak should not be ascribed as paraformaldehyde depolymerization/volatilization (144 $^\circ\text{C}$), since no residue was detected in FT-IR (Fig. 2)⁷. An endothermic event at 166–180 $^\circ\text{C}$ can be seen, probably related to the melting of oligomeric fractions with methylene-bridges. The endothermic peak related to methyl urea

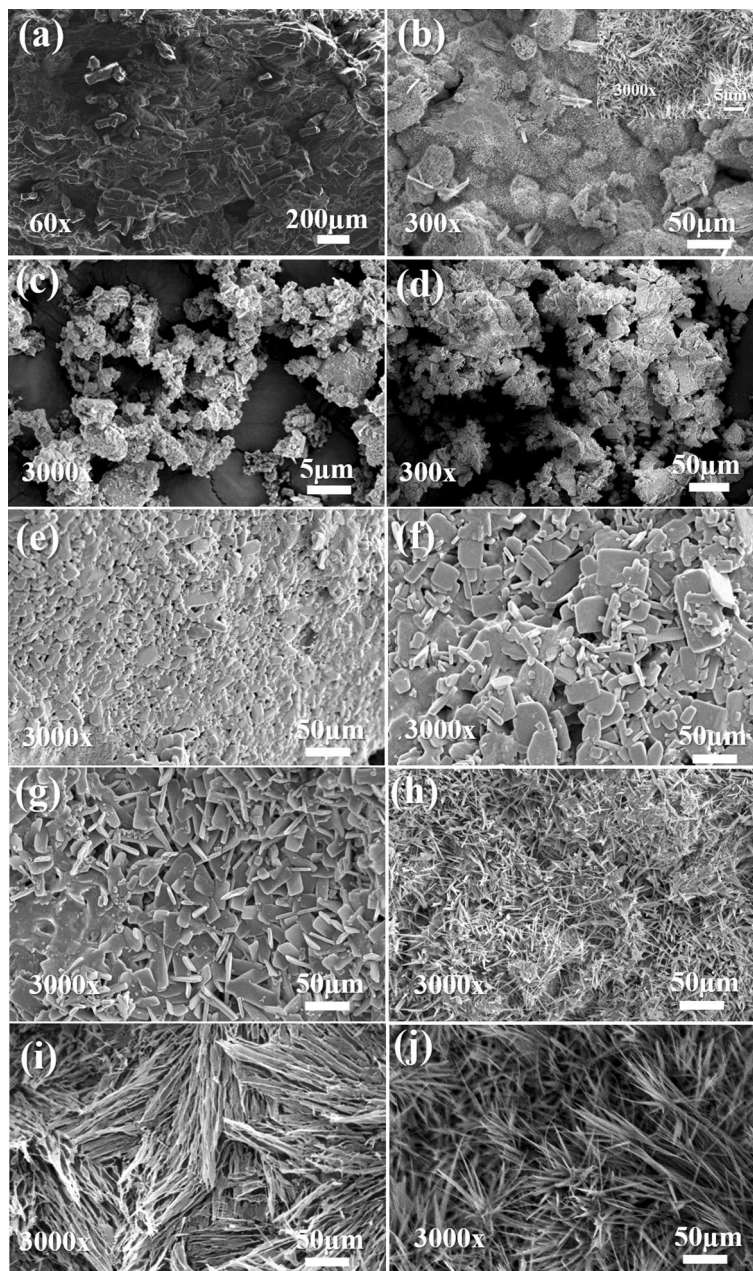


Figure 1. SEM images with its magnifications of (a) pure urea, (b) pure polymer UF, (c) ZnO, (d) ZnSO₄, (e) UFZO 0.5, (f) UFZO 1, (g) UFZO 2, (h) UFZS 0.5, (i) UFZS 1 and (j) UFZS 2. (UF = pure polymer, UFZO = composites with ZnO and UFZS composites with ZnSO₄).

bonds in UF (180.6 °C) has shifted to lower temperatures. DSC analysis showed that Zn sources might play a role in catalyzing the thermal degradation, with endothermic peaks shifted to lower temperatures, indicating lower thermal stability. The complete decomposition of the compound occurs over 200 °C.

Comparing DSC results with thermogravimetry (TG and DTG) (Fig. 4c–f), it is possible to identify that urea degrades in three stages (peaks at 182, 237, 292 °C), and paraformaldehyde has a single stage (154 °C). The UF profile shows that the endothermic peak in DSC from 115 to 122 °C corresponds to a degradation mechanism, thus confirming the correlation to bridge breaking in oligomeric fractions. The next three stages (centered at 235, 287, and 330 °C) are probably related to the loss of functional groups of different chemical natures and energy costs²³. UFZO composites behave very closely to pure UF; however, in the 2nd degradation stage it shifts to lower temperatures, suggesting the breakdown of the H-bonds. UFZO 2 (Fig. 4c) has an additional degradation event (183 °C) suggesting chains with intermediary lengths. The residual mass increases according to the Zn content. It supports that Zn has acted as a catalyst for breaking chain interactions. Nevertheless, UFZS materials have gradual decomposition depending on the polycondensation degree. These composites show only 3 stages of

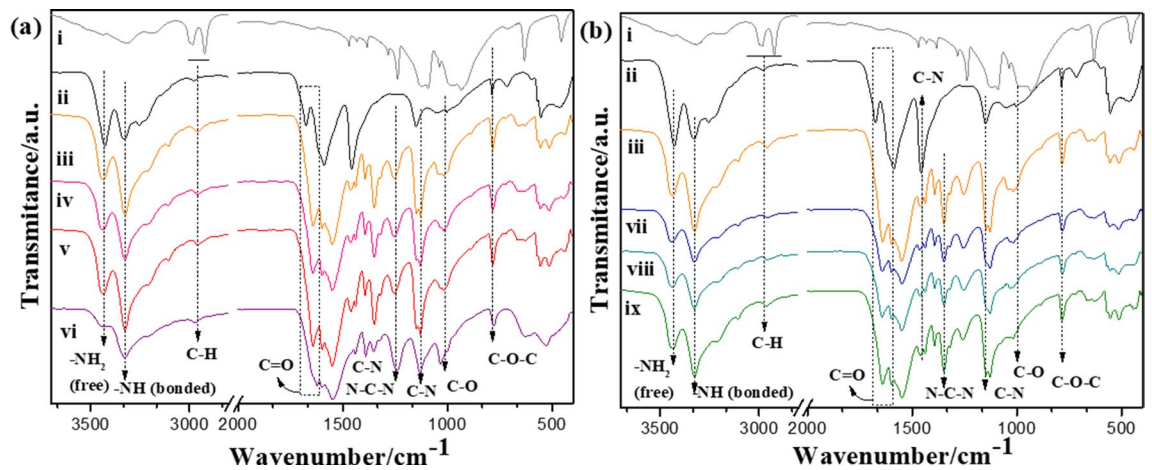


Figure 2. Normalized FTIR spectra in (a): (i) paraformaldehyde, (ii) urea (iii) pure polymer UF, (iv) UFZO 0.5, (v) UFZO 1, (vi) UFZO 2 and in (b): (vii) UFZS 0.5, (viii) UFZS 1 and (ix) UFZS 2.

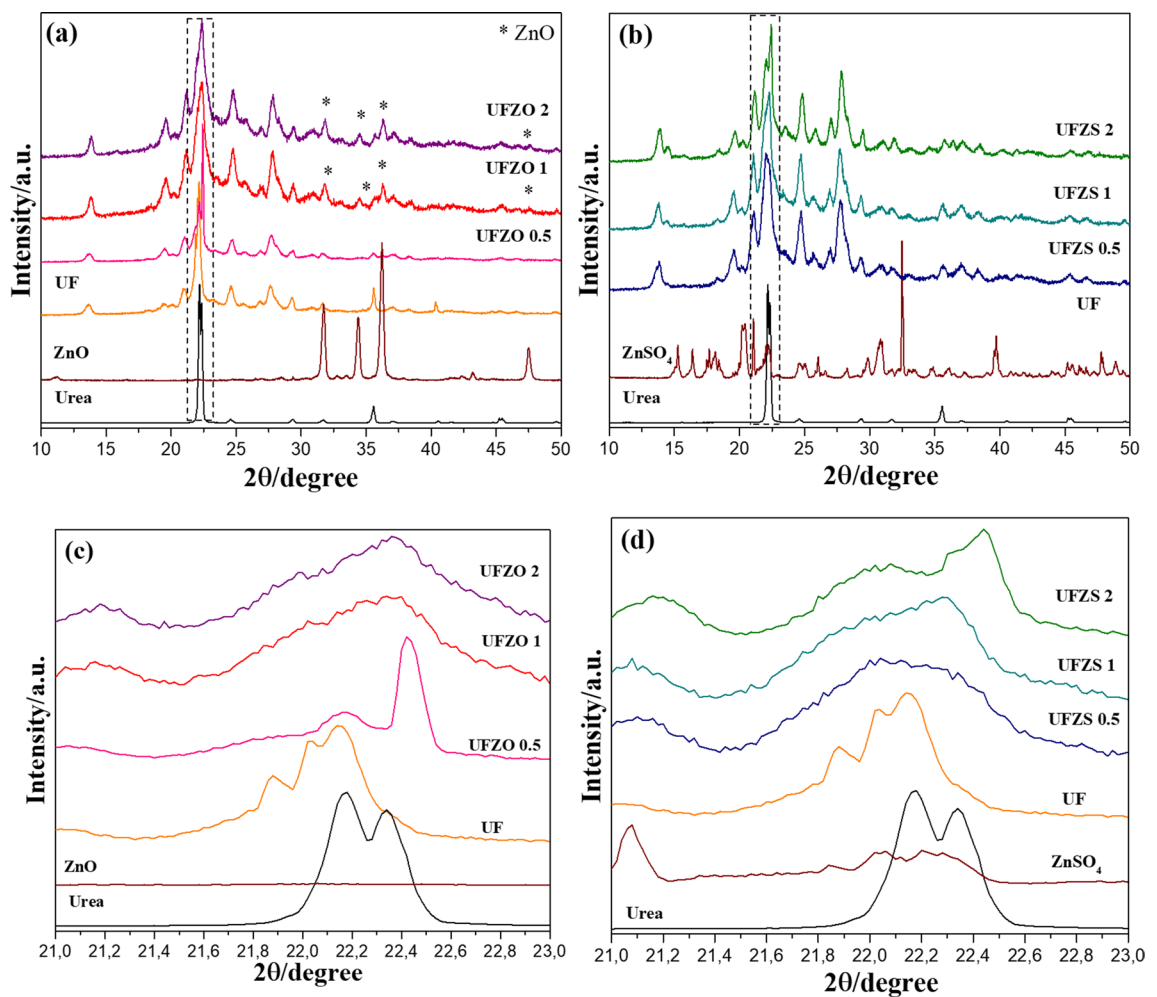


Figure 3. Normalized XRD pattern of Ur and UF with (a) ZnO, UFZO 0.5, UFZO 1, UFZO 2, (b) ZnSO₄, UFZS 0.5, UFZS 1 and UFZS 2 (c, d) amplification the area at $2\theta = 21\text{--}23^\circ$.

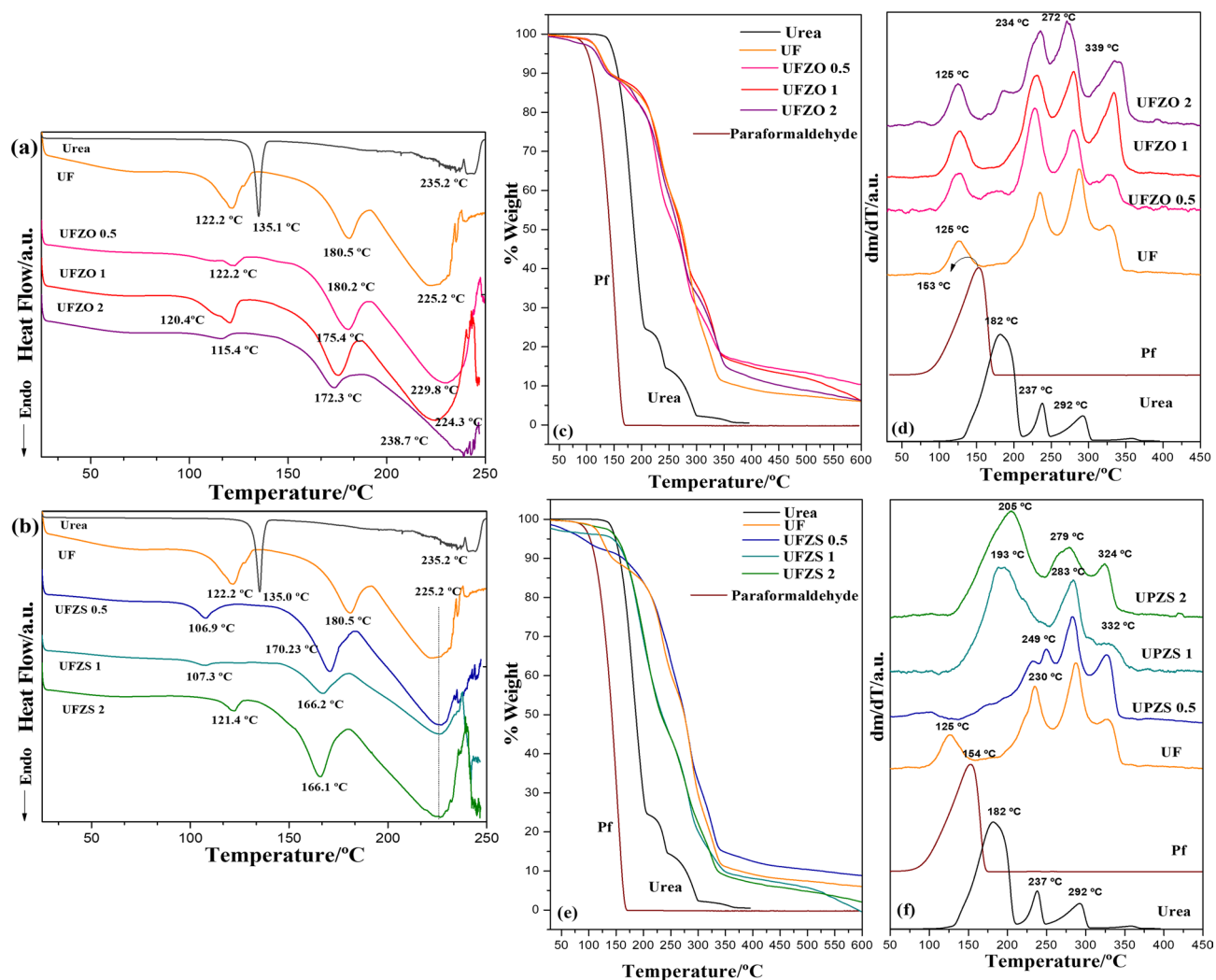


Figure 4. Thermal analysis: DSC curves of urea, UF, (a) UFZO composites, (b) UFZS at a heating rate of 10 °C/min and (c–f) TGA of urea, UF, (c) UFZO composites, (d) UFZS obtained by TGA and expressed as the derivative (DTG) (e, f).

degradation instead of 4, starting over 190 °C. UFZS 0.5 is closer to pure UF, while UFZS 1 and 2 had their 1st stage dislocated to lower temperatures with a major area of degradation compared to the subsequent events. As seen in XRD, ZnSO_4 may be intercalated to the UF, changing the crystallinity and reducing the thermal stability. The residual UFZS was also dependent on the ZnSO_4 content. Each Zn source led to different thermal behaviors, probably due to their different effects in crystallization.

The reaction extension and the effect of Zn sources has been verified by NMR techniques. ^1H - and ^{13}C -NMR and are shown in Figs. 5 and 6. Figure 5 a and b show the full spectra of ^1H NMR from 7.00 to 2.00 ppm. There are substantial regions of monosubstituted amide ($-\text{CONHCH}_2-$) at 7.00–5.80 ppm, nonsubstituted amide ($-\text{CONH}_2$) at 5.80–5.40 ppm, hydroxyl ($-\text{OH}$) at 5.30–5.00 ppm, and methylene ($-\text{CH}_2-$) signal at 5.00–4.10 ppm²⁹. All materials have two signals at 6.83 and 6.60 ppm assigned to mono- and di-(hydroxymethyl) urea (Fig. S3 b). These signals confirmed the expected H-bond formation with the ($-\text{CONHCH}_2-$) groups, as observed in the FTIR results. Multiple peaks at 5.61 indicate various chemical environments attached to the terminal $-\text{CONH}_2$ group. Only $-\text{CONH}_2$ attached to the smaller oligomer chains (Fig. S3 c) tends to have a higher chemical shift due to the inductive effect. Various oxygen atoms along the oligomer backbone could attract electron density from the hydrogen of $-\text{CONH}_2$, since UF has a small peak at 5.76 ppm. For other materials as UFZO and UFZS composites, the higher intensity of the signal at 5.61 ppm implies that all materials had a proportion of the $-\text{CONH}_2$ group attached to the long chains than that to the short ones. The strong peak at 5.41 ppm is assigned to $-\text{NH}_2$ group of free urea, indicating the type of urea:urea-formaldehyde polymer structure. Multiple signals (4.52–4.15 ppm) are assigned to ($-\text{CH}_2-$) methylene in ($-\text{NHCH}_2\text{NH}-$) and in hydroxymethyl ($\text{HOCH}_2\text{NH}-$) as illustrated in Fig. S3 d. A shoulder at 4.46 ppm is due to the presence of oxygen in the groups, which became smooth for the composites compared to pure UF, indicating that Zn guided the urea condensation to better dispersion, as shown in Fig. S3 c. It suggests that the formation of long UF chains is suppressed in composites. The increase of $-\text{OCH}_3$ peak (3.16 ppm) (obtained by reaction of formaldehyde at the end of the polymer chain) in composites suggest that there are more terminal groups, thus, smaller chains, which supports

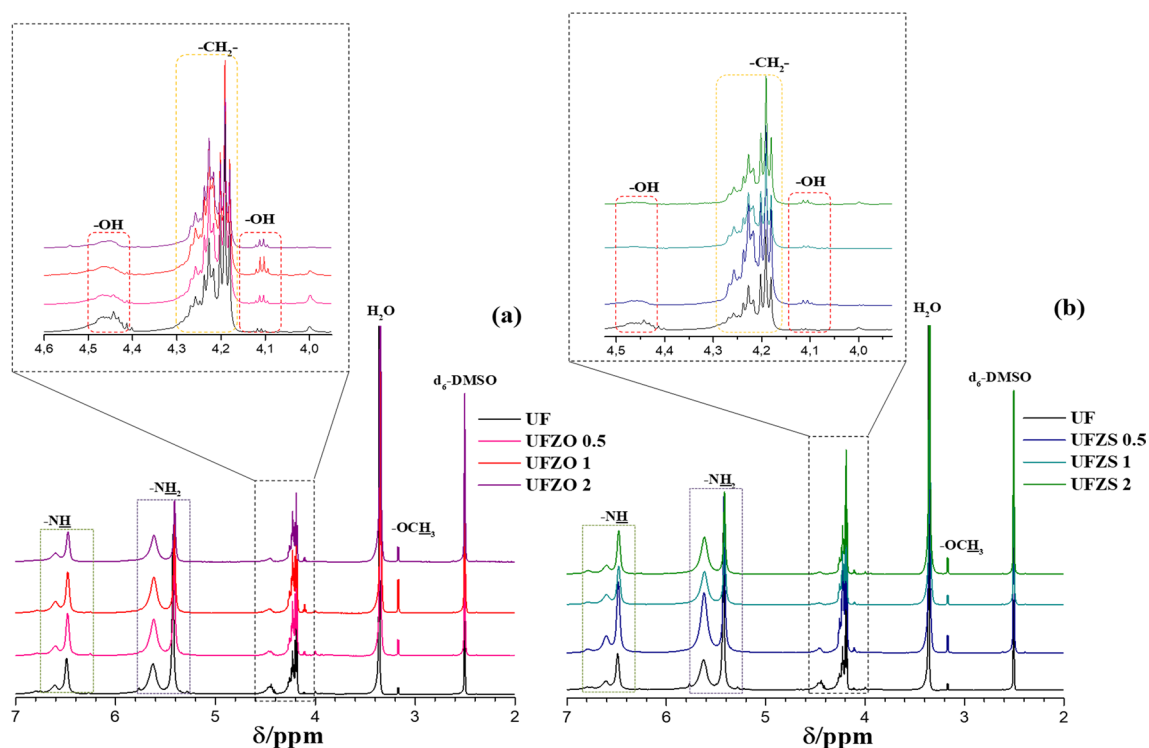


Figure 5. ^1H NMR spectra of UF and composites (a) UFZO and (b) UFZS solubilized in d_6 -DMSO.

the proposed Zn effect. The hydroxyls remain in all materials as evidenced by the signals from 4.0–4.12 ppm, further corroborating with the suggested formation of hydroxyl methyl urea structures along the main chain of urea-formaldehyde²⁶. Urea-formaldehyde polymers cannot be described by a single formula³³ and all analyses were done to approximate as much as possible to the real expected compound.

^{13}C NMR is shown in Fig. 6, where the signals for urea carbonyls are assigned according to the substitution differences. No unreacted urea is seen in all materials, confirming that all urea was consumed in the polycondensation. The chemical assignments between 160 and 156 ppm are attributed to mono-, di-, and trisubstituted amides. Furthermore, the $\text{C}=\text{O}$ signals at 159.5 ppm indicate the formation of H-bonds as shown in Fig. 6c, and it agrees to the ^1H NMR and FTIR^{27,29}. Di-substituted urea appears at 157–158 ppm and monosubstituted urea at 158–159 ppm²⁸. All carbonyl signals shifted in due to Zn particles that disturb the carbon nucleus and modify its resonance. Therefore, all results indicate the formation of linear oligomers (with different lengths), and the formation of H-bonds between $\text{C}=\text{O}$ and $\text{N}-\text{H}$ groups in this kind of structure, leading to crystallization as verified by XRD pattern.

Figure 7a illustrates the urea release in water of pure urea and UF compared to all composites at 25 °C. It can be seen that almost all materials release more than 25% of the N content within 24 h. Some commercial urea brands show some controlled release behavior alone, as observed in Fig. 7. A small portion of formaldehyde might have been added to help the granulation process. Interestingly, when analyzing the FTIR of pure urea, the presence of this compound can be seen by the enlargement of the NH stretching of urea as well as the duplication of NH signals, which also indicate some interaction of NH of urea and OH band of formaldehyde form in the granule. Therefore, UF polymers presented a small difference compared to pure urea in the release test in water medium. As discussed, it is expected that the materials have a more controlled release compared to pure urea, due to the formation of small molecules of substituted urea, as observed in our experiments. About 20–30% of the urea has remained in the materials after 140 h, while pure urea is completely solubilized. UF fertilizers are already recommended to fertilize perennial plants, such as forests, fruit plants, and lawns, which require long N release³⁰. A new range of crops could be targeted to N fertilization with the studied materials. The different profiles of release from the composites and UF is due to the intercalated Zn particles. Figure 7b shows Zn release behavior from the composites and pure sources (ZnO and ZnSO_4). In contrast to ZnO , which has no solubilization in the period of the experiment, UFZO materials released 30–40% of Zn after 140 h. The dispersion effect increases the ZnO solubilization, in a similar effect as observed for hydroxyapatite powders in urea³⁴. On the other hand, ZnSO_4 results in a controlled-release in the composites, instead of the fast delivery observed from the highly soluble pure ZnSO_4 salt. The increased interaction of ZnSO_4 with the UF structure can explain this behavior, as seen by the thermoanalysis and FTIR. It also corroborates that the ZnSO_4 salt is solubilized during synthesis and re-precipitates within the UF structure, being highly intercalated and dispersed in the matrix and acting as physical and chemical barrier for hydrogen bond formation.

The incubation in soil for 42 days reveals the behavior of N in real conditions and the effects of each Zn source, as shown in Fig. 8. In this experiment, N transformation was monitored from urea hydrolysis, assessing the available $\text{N}-\text{NH}_4^+$ in soil and the loss of N by NH_3 volatilization. N-release rate from UF and the composites was

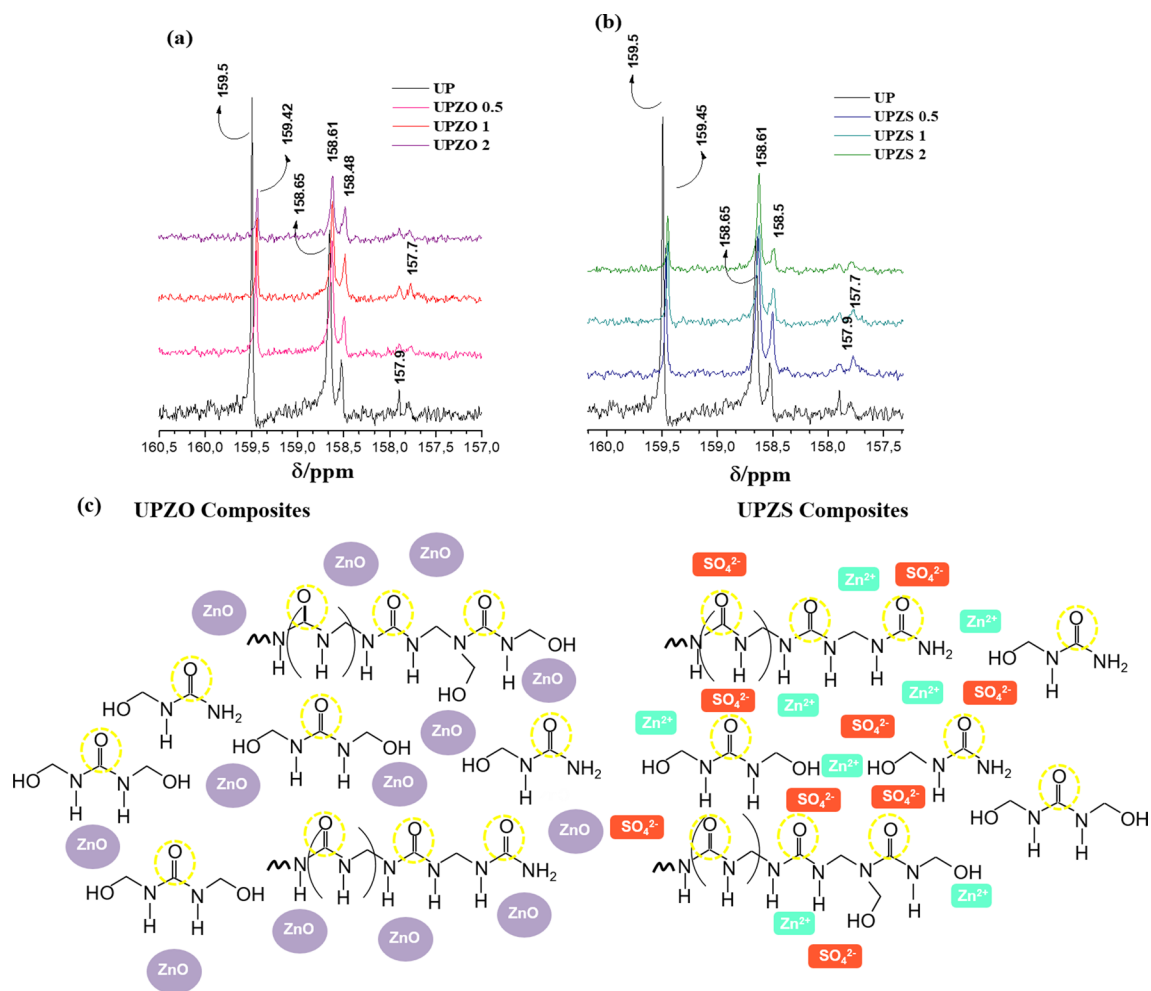


Figure 6. Amplification spectra of ^{13}C NMR 160–157 ppm of composites (a) UFZO and (b) UFZS solubilized in $\text{DMSO}-d_6$ and molecular structure proposed for the interaction of Zn particles with the polymers as well as the different medium of carbonyl groups. Molecular structure created using software Microsoft PowerPoint 2016 version.

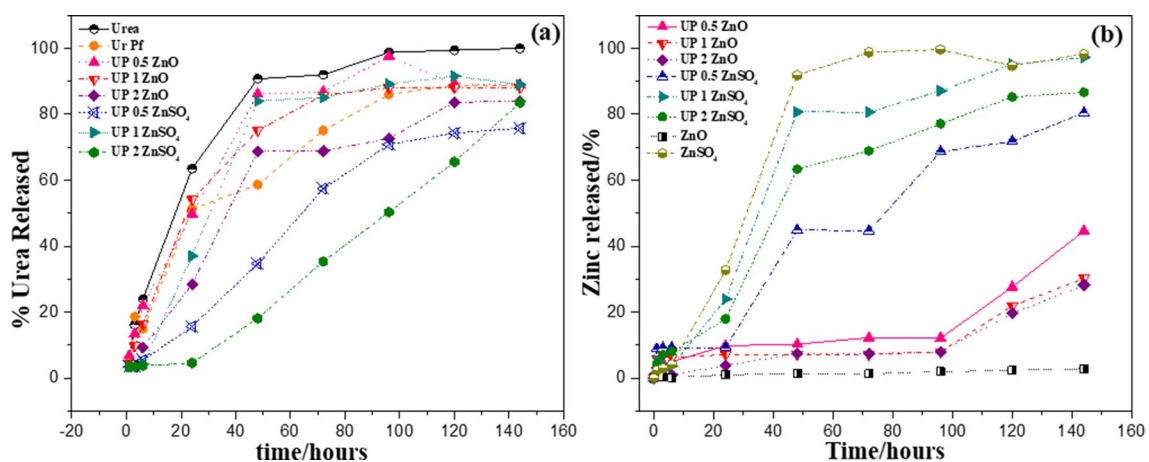


Figure 7. Release rates for (a) urea species and (b) zinc of materials cultivated in still water.

slower in the first 7 days and then gradually raised up, while pure urea displayed a fast initial release and started to decline after 14 days. UFZS 0.5 and 1 showed the highest NH_4^+ values after 14 days among the composites, but still lower than pure urea. This suggests that ZnSO_4 is favoring the N release from the UF structure. However,

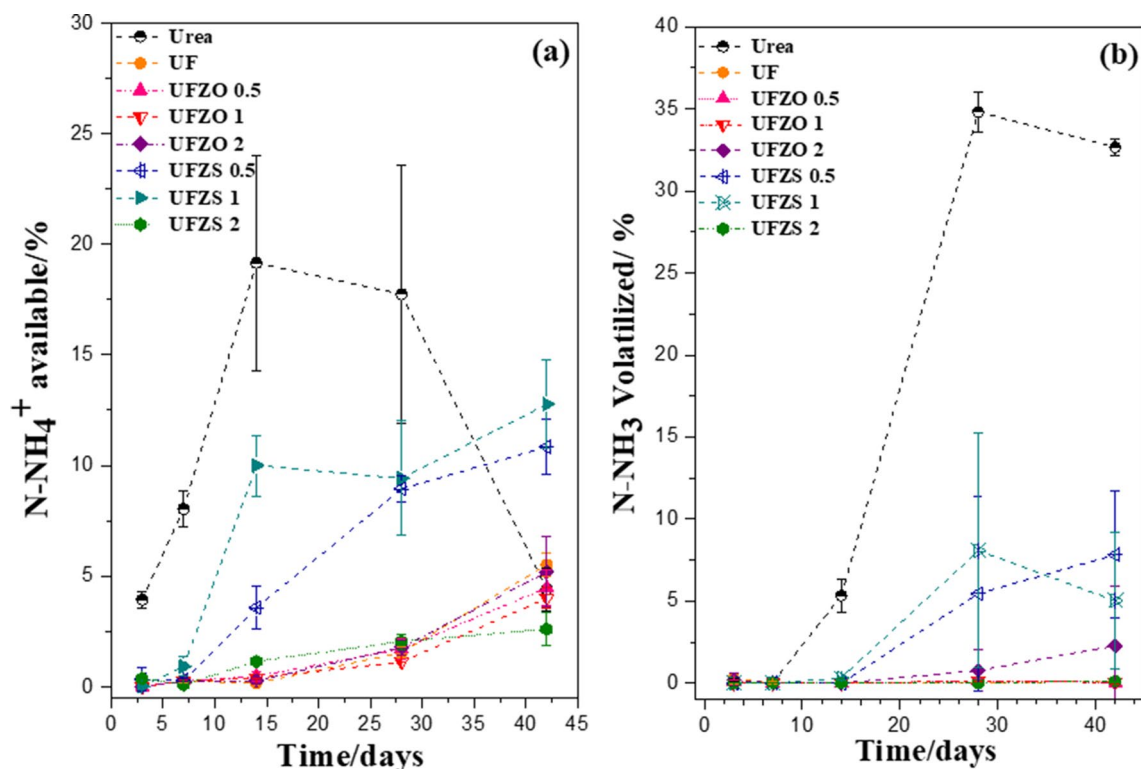


Figure 8. N recovery from the fertilizers as (a) $N-NH_4^+$ available and (b) $N-NH_3$ volatilized for each fertilizer treatment over the 42-day incubation period.

the same result was not observed for UFZS 2, which had no release of urea in water medium (Fig. 7a). Pure urea and UFZO composites also presented low N release in soil (<5% of total N), indicating a need for longer periods (more than 42 days) to fully release the structural N, typical for slow-release fertilizers. UF presents a lower solubility compared to pure urea as its structure is more complex, with different chain lengths and substituents, slowing down the hydrolysis rate³⁵.

Therefore, most of the N in the composites could be released with longer incubation time. The first N released to soil is possibly from low length compounds (mono and hydroxymethyl ureas or mono- and di- substituted ureas) while the longest release is due to hydrolysis of longer chains. Zn reduces the interaction between chains, especially $ZnSO_4$ by its lower pH compared to ZnO. This behavior is verified by Zhang et al.¹¹, in their NPK composites. With the highest profile of NH_4^+ release from UFZS0.5 and UFZS1, they also achieved the highest volatilized NH_3 values among the composites, with 7.5 and 5.5%, respectively, which was still lower than pure urea (35%) in 28 days.

Table 1 shows the N application in soil that has been lost (volatilized) as NH_3 and is still available after 42 days of incubation. N-residual corresponds to the nutrient still in the fertilizer matrix or immobilized by the soil microbiota. Although a small fraction could be lost by the formation of other N oxides that were not measured, they were considered less important in the experimental context. The results confirm the low availability of $N-NH_4^+$ species after 42 days of urea incubation in soil. This low efficiency is attributed to the high NH_3 volatility, which in this study was 32% by the end of the experiment^{36–38}. As previously discussed, although urea provides high availability of $N-NH_4^+$ 14 days after incubation, the available N for plant absorption considerably reduces after 28 days (Fig. 8a). The reduction in $N-NH_4^+$ is a consequence of its transformation to NH_3 and subsequent loss through volatilization. In this way, the availability of N from urea fertilizer is concentrated in a short period of time, which reduces the use/absorption by the plants that require the nutrient throughout their vegetative and reproductive cycles. This result highlights the low agronomic efficiency of the urea when applied to the soil in these conditions^{35,36}. This is one of the reasons for the effort in the search for a fertilizer capable of supplying N in a more regular and constant way, that can be synchronized with the plants' demands.

Regarding this purpose, the N release profiles of the composites UFZS 0.5 and 1 indicate their potential use, considering the controlled N release, lower NH_3 volatilization and greater NH_4^+ availability after 42 days of incubation, compared to pure urea (Fig. 8 and Table 1). By delivering N in a slower manner and avoiding its loss, the composites are less damaging to the environment and more efficient in the longer term. In addition, these materials provide the possibility of joint supply of N and Zn to plants, besides the effect of the interaction between urea-formaldehyde with Zn sources (ZnO and $ZnSO_4$), which proved to be strategic to modulate the polymer chain growth and improve the Zn accessibility.

Fertilizers	N-NH ₄ ⁺ available in soil	N-NH ₃ volatilized
	%	
Urea	4.40 b	32.7 d
UF	5.52 b	0.13 a
UFZO 0.5	4.47 b	0.05 a
UFZO 1	4.00 bc	0.05 a
UFZO 2	5.18 b	2.27 ab
UFZS 0.5	10.84 a	7.82 c
UFZS 1	12.77 a	7.41 bc
UFZS 2	2.60 c	0.13 a

Table 1. N recovery from the fertilizers as N-NH₄⁺ available, and N-NH₃ volatilized, after 42 days soil incubation. The data shows average values of each N fraction derived of total N applied to the soil as urea, UF or composites. (UF = pure polymers, UFZO = composites with ZnO and UFZS composites with ZnSO₄). The estimative of N recovery percentage was calculated by the total N content present in the composites (10 mg of N) subtracted by the N content converted into ammonium or ammonia extracted from the soil (determined by colorimetric or titration method). *Values within a column followed by the same letter do not differ significantly (Tukey's test; P < 0.05) with n = 4 replicates.

Materials	Name	% Nutrient	
		N	Zn
Urea	Ur	45	–
UrPf 1:0.5	UF	40.71	–
UrPfZnO 0.5	UFZO 0.5	40.07	0.456
UrPfZnO 1	UFZO 1	41.40	0.732
UrPfZnO 2	UFZO 2	40.43	1.440
UrPfZnSO ₄ 0.5	UFZS 0.5	43.70	0.352
UrPfZnSO ₄ 1	UFZS 1	44.52	0.635
UrPfZnSO ₄ 2	UFZS 2	37.96	1.880

Table 2. List of named composites with their final composition.

Methods

Materials. Urea (Synth, Brazil) and paraformaldehyde (Sigma-Aldrich, USA) (both chemical structures displayed in Fig. S3 a), ZnO and ZnSO₄·7H₂O (Synth, Brazil) were used for the materials' production. Urea and ZnSO₄ salt were previously milled to a size range of ≤ 300 μm using a TE-330 hammer mill (Tecnal, Brazil). The ZnO powder was sieved in 300 μm to standardize the initial particle size.

Preparation of materials. UF was prepared following the molar ratio of 1:0.5 between urea and paraformaldehyde. The reagents were processed using a torque rheometer (Polylab RHEODRIVE Rheomix mixer and OS4) under 60 rpm and 90 °C for 10 min to mix-melt the reagents. For the UF/Zn composites, all components were used as powders with standardized particle sizes of ~ 300 μm, previously mixed in plastic bags to achieve homogeneity before being submitted to the mixed-melting process, maintaining the same molar ratio of urea: paraformaldehyde as described. The Zn was added in varying proportions to the UF, namely 0.5, 0.7, and 1.45% (wt.%) of Zn for both ZnO and ZnSO₄. After mixing, the samples were cured in an oven at 80 °C for 12 h and before storage all samples were classified using a sieve of < 500 μm. No float was observed during the synthesis once urea melting helped in aggregating all solids together, followed by the homogenization reached by the mixture in the rheometer machine. The name and the total percentage of nutrients are described in Table 2.

Characterizations. The composites' morphologies were characterized by scanning electron microscopy (SEM) using a JSM6510 microscope (JEOL) using the secondary electron mode. Thermal analysis was conducted at the range of 25 °C to 600 °C using a Q500 analyzer (TA Instruments, New Castle, DE, USA) with a heating rate of 10 °C min⁻¹ under nitrogen atmosphere. For the differential scanning calorimetry (DSC), samples were heated from 25 to 250 °C in a DSC Q100 (TA Instruments, USA) under nitrogen atmosphere. Fourier Transform Infrared was carried out in an FTIR spectrophotometer VERTEX 70 (Bruker Corporation) with ATR technique. Proton and carbon nuclear magnetic resonance (¹H- and ¹³C- NMR) spectra were obtained on a 600 MHz Avance III HD Bruker spectrometer using dimethyl sulfoxide (DMSO-d₆) as a solvent and tetramethylsilane (TMS) as the internal reference.

Soil characteristics									
pH	CEC ^a	Organic C	Sand	Silt	Clay	WHC ^b	N	Zn	Urease activity
	(cmol _c kg ⁻¹)	(g kg ⁻¹)						(mg kg ⁻¹)	(mg N kg ⁻¹ h ⁻¹)
5.0	4.2	7.0	433	35	532	200	1.06	0.51	7.1

Table 3. Chemical and physical properties of the studied soils. ^aCEC, cation exchange capacity. ^bWHC, water-holding capacity.

Release tests in solution. The composites were submitted to test for both urea and Zn release as a function of time. The release rate in water was determined by adding the samples to beakers and gently stirring for 5 days using an orbital shaker at 50 rpm (Thermo scientific) and 25 °C. To determine the dissolution of urea and zinc, aliquots of 2 mL were collected and centrifuged (15 min at 14,000 rpm, MiniSpin Plus) at different time intervals (three times in the first day and after once a day), over 5 days. The maximum level of urea added in each experiment was the same (1250 mg L⁻¹); that is, different mass values for the composites were calculated so that each experiment had the same amount of urea. For comparison, a test with pure urea, ZnO and ZnSO₄ was also performed as a control experiment. The determination of urea concentration in solution was done by UV–vis spectrophotometry (Shimadzu-1601PC), according to the method of Tomaszewska and Jarosiewicz³⁹, and Giroto et al.⁸. Zn release rate determination was performed using atomic absorption spectrophotometry using a part of the aliquots (PinAAcle 900 T- PerkinElmer). Thus, a curve of urea and zinc concentration in solution versus release time was obtained.

Nitrogen mineralization in soil. Nitrogen transformations in soil to ammonium and ammonia volatilization were investigated in an Oxisol (Red-Yellow Oxisol which was collected at 20 cm depth at a pasture site in São Carlos, Brazil), which was characterized according to its physical and chemical aspects^{40–42}. Details of the soil characteristics are provided in Table 3. The soil samples were air-dried and crushed to pass through a 2 mm screen before use. Soil samples (10 g) were incubated using an incubation system with the tested fertilizers at a 1000:1 g g⁻¹ ratio of soil:N, placed in 125 mL polyethylene screw-cap bottles as Ur, UF and composites (UFZO 0.5, 1 and 2) or (UFZS 0.5, 1 and, 2), as described by Guimarães et al.³⁶ and Giroto et al.⁸. Samples were incubated for 3, 7, 14, 28 and 42 days under controlled temperature (25 °C) and humidity (60% WHC).

Analyzes were performed after each 3, 7, 14, 28 and 42 days. Determinations were carried out via volatilization⁴³ and the soil mineralization of N-NH₄⁺⁴⁴ followed the description used by Giroto et al.³⁷. Volatilized NH₃ was quantified by titration of boric acid with HCl (0.01 mol L⁻¹). Mineral N produced during incubation was extracted by shaking the soil sample with 100 mL of KCl (1 mol L⁻¹) containing phenyl mercuric acetate (5 mg L⁻¹) as a urease inhibitor (soil:solution ratio of 1:10). Afterwards, the suspension was stirred for 1 h and filtered through filter paper (diameter 12.5 cm Whatman no. 42 filter paper (GEHealthcare, Buckinghamshire, UK)). The resulting soil extract was stored in 100 mL polyethylene bottles at 5 °C. The ammonium (NH₄⁺) levels in the soil extracts were determined by the colorimetric methods of Kempers and Zweers⁴⁴. The contents recovered in each N fraction (NH₄⁺ and NH₃) were expressed as percentages in relation to the N added to soil in the form of urea or composite.

Analysis of variance (ANOVA) was done for the differences among treatments by total recovery as NH₃ volatilized and exchangeable NH₄⁺ after aerobic incubation and when the F test was significant, differences among treatments were compared by the Tukey test (P < 0.05).

Conclusions

The results of this study showed that the formation of the UF polymers was affected by the loading of Zn in composites during the synthesis with no dependence on a specific Zn source. XRD analysis clearly showed the distinction in the crystallinity of the materials with the addition of Zn, which was also verified in the nutrients released in water medium, promoting the controlled release of nitrogen in all composites. Zn sources featured a different solubilization behavior in the release test. ZnSO₄, a soluble source, had a controlled delivery due to its dispersion throughout the UF composite, as verified by XRD and SEM analysis. On the other hand, the low solubility of ZnO was enhanced in the composites, with a better performance after 4 days of water immersion, releasing 40% of Zn at 7 days. ¹H- and ¹³C- NMR analyses showed the Zn particles have unsettled the arrangement of the polymer chains, which prevented the length growth of the polymer chains compared to the pure UF. This study proved the feasibility of the production and applications of UF loaded with Zn, as slow-release fertilizers or other products in agriculture, showing the beneficial effects for both nutrients, i.e., reduces N volatilization and increases Zn bio-availability.

Received: 5 February 2021; Accepted: 23 March 2021

Published online: 07 April 2021

References

1. Neamațu, C., Popescu, M., Oancea, F. & Dima, ȘO. Synthesis optimization and characterization of microencapsulated N-P-K Slow-release fertilizers. *Open Chem.* **13**, 813–823 (2015).

2. Pang, W. *et al.* Preparation of microcapsules of slow-release NPK compound fertilizer and the release characteristics. *J. Braz. Chem. Soc.* **29**, 2397–2404 (2018).
3. Silva, D. R. G. & Lopes, A. S. Princípios Básicos Para Formulação E Mistura De Fertilizantes. *Ed. UFPA* **89**, 1–46 (2012).
4. Janmohammadi, M., Fattahi, M., Sabaghnia, N. & Nouraein, M. Effects of metal oxides and urea fertilizer on agronomic traits of safflower. *Sci. Agric. Bohem.* **49**, 153–163 (2018).
5. Jiao, G. J., Xu, Q., Cao, S. L., Peng, P. & She, D. Controlled-release fertilizer with lignin used to trap urea/hydroxymethylurea/urea-formaldehyde polymers. *BioResources* **13**, 1711–1728 (2018).
6. Dimkpa, C. O. *et al.* Facile Coating of Urea With Low-Dose ZnO Nanoparticles promotes wheat performance and enhances Zn uptake under drought stress. *Front. Plant Sci.* **11**, 1–12 (2020).
7. Yamamoto, C. F., Pereira, E. I., Mattoso, L. H. C., Matsunaka, T. & Ribeiro, C. Slow release fertilizers based on urea/urea-formaldehyde polymer nanocomposites. *Chem. Eng. J.* **287**, 390–397 (2016).
8. Giroto, A. S. & Ribeiro, G. G. F. G. C. A. Novel, simple route to produce urea: urea – formaldehyde composites for controlled release of fertilizers. *J. Polym. Environ.* **26**, 2448–2458 (2018).
9. Guo, J. X. *et al.* Effects of soil zinc availability, nitrogen fertilizer rate and zinc fertilizer application method on zinc biofortification of rice. *J. Agric. Sci.* **154**, 584–597 (2016).
10. Yang, J., Kong, X., Xu, D., Xie, W. & Wang, X. Evolution of the polydispersity of ammonium polyphosphate in a reactive extrusion process: Polycondensation mechanism and kinetics. *Chem. Eng. J.* **359**, 1453–1462 (2019).
11. Zhang, W. *et al.* Biodegradable urea-formaldehyde/PBS and Its ternary nanocomposite prepared by a novel and scalable reactive extrusion process for slow-release applications in agriculture. *J. Agric. Food Chem.* **68**, 4595–4606 (2020).
12. Trenkel, M. E. *Controlled-Release and Stabilized Fertilizers in Agriculture. Libro Fertilizantes* (1997).
13. Guo, Y. *et al.* Modeling and optimizing the synthesis of urea-formaldehyde fertilizers and analyses of factors affecting these processes. *Sci. Rep.* **8**, 1–9 (2018).
14. Wang, H. *et al.* Characterization of the low molar ratio urea-formaldehyde resin with ¹³C NMR and ESI-MS: Negative effects of the post-added urea on the urea-formaldehyde polymers. *Polymers (Basel)*. **10**, 1 (2018).
15. Zhao, P., Yang, F., Sui, F., Wang, Q. & Liu, H. Effect of nitrogen fertilizers on zinc absorption and translocation in winter wheat. *J. Plant Nutr.* **39**, 1311–1318 (2016).
16. Daoudi, M. & Singh, R. Effect of Nitrogen and Sulphur on Growth and Yield of Hybrid Maize (*Zea mays* L.). *Int. J. Curr. Microbiol. Appl. Sci.* **6**, 1930–1935 (2017).
17. Salehin, F. & Rahman, S. Effects of zinc and nitrogen fertilizer and their application method on yield and yield components of *Phaseolus vulgaris* L. *J. Agric. Sci.* **03**, 9–13 (2012).
18. Cakmak, I. Enrichment of cereal grains with zinc: Agronomic or genetic biofortification?. *Plant Soil* **302**, 1–17 (2008).
19. Alvarez, J. M. & Rico, M. I. Effects of zinc complexes on the distribution of zinc in calcareous soil and zinc uptake by maize. *J. Agric. Food Chem.* **51**, 5760–5767 (2003).
20. Sun, H. *et al.* Development of ZnO Nanoparticles as an Efficient Zn Fertilizer: Using Synchrotron-Based Techniques and Laser Ablation to Examine Elemental Distribution in Wheat Grain. *J. Agric. Food Chem.* **68**, 5068–5075 (2020).
21. Irfan, M., Khan Niazi, M. B., Hussain, A., Farooq, W. & Zia, M. H. Synthesis and characterization of zinc-coated urea fertilizer. *J. Plant Nutr.* **41**, 1625–1635 (2018).
22. Pereira, E. I. *et al.* Controlled urea release employing nanocomposites increases the efficiency of nitrogen use by forage. *ACS Sustain. Chem. Eng.* **5**, 9993–10001 (2017).
23. González-Hurtado, M., Rieumont-Briones, J., Castro-González, L. M., Zumeta-Dube, I. & Galano, A. Combined experimental-theoretical investigation on the interactions of Diuron with a urea-formaldehyde matrix: Implications for its use as an ‘intelligent pesticide’. *Chem. Pap.* **71**, 2495–2503 (2017).
24. Zorba, T., Papadopoulou, E., Hatjiissaak, A., Paraskevopoulos, K. M. & Chrissafis, K. Urea-formaldehyde resins characterized by thermal analysis and FTIR method. *J. Therm. Anal. Calorim.* **92**, 29–33 (2008).
25. Mattos, Ed. C., Viganó, I., Dutra, R. D. C. L., Diniz, M. F. & Iha, K. Aplicação de metodologias FTIR de transmissão e fotoacústica à caracterização de materiais altamente energéticos: parte II. *Quim. Nova* **25**, 722–728 (2002).
26. Jada, S. S. The structure of urea—formaldehyde resins. *J. Appl. Polym. Sci.* **35**, 1573–1592 (1988).
27. Christjanson, P., Pehk, T. & Siimer, K. Hydroxymethylation and polycondensation reactions in urea-formaldehyde resin synthesis. *J. Appl. Polym. Sci.* **100**, 1673–1680 (2006).
28. Pereira, P. *et al.* Copolymerization of UF resins with dimethylurea for improving storage stability without impairing adhesive performance. *Materials (Basel)*. **11**, 1 (2018).
29. Wibowo, E. S., Park, B. D. & Causin, V. Hydrogen-bond-induced crystallization in low-molar-ratio urea-formaldehyde resins during synthesis. *Ind. Eng. Chem. Res.* **59**, 13095–13104 (2020).
30. Xiang, Y. *et al.* Granular, slow-release fertilizer from urea-formaldehyde, ammonium polyphosphate, and amorphous silica gel: a new strategy using cold extrusion. *J. Agric. Food Chem.* **66**, 7606–7615 (2018).
31. Qu, P., Huang, H., Wu, G., Sun, E. & Chang, Z. Hydrolyzed soy protein isolates modified urea-formaldehyde resins as adhesives and its biodegradability. *J. Adhes. Sci. Technol.* **29**, 2381–2398 (2015).
32. Khonakdar Dazmiri, M., Valizadeh Kiamahalleh, M., Dorieh, A. & Pizzi, A. Effect of the initial F/U molar ratio in urea-formaldehyde resins synthesis and its influence on the performance of medium density fiberboard bonded with them. *Int. J. Adhes. Adhes.* **95**, 1 (2019).
33. Dankelman, W. *et al.* Modern methods for the analysis of urea formaldehyde resins. *Die Angew. Makromol. Chemie* **54**, 187–201 (1976).
34. Giroto, A. S., Fidélis, S. C. & Ribeiro, C. Controlled release from hydroxyapatite nanoparticles incorporated into biodegradable, soluble host matrixes. *RSC Adv.* **5**, 104179–104186 (2015).
35. Giroto, A. S., Guimarães, G. G. F., Foschini, M. & Ribeiro, C. Role of slow-release nanocomposite fertilizers on nitrogen and phosphate availability in soil. *Sci. Rep.* **7**, 46032 (2017).
36. Guimarães, G. G. F., Mulvaney, R. L., Khan, S. A., Cantarutti, R. B. & Silva, A. M. Comparison of urease inhibitor N-(n-butyl) thiophosphoric triamide and oxidized charcoal for conserving urea-N in soil. *J. Plant Nutr. Soil Sci.* **179**, 520–528 (2016).
37. Giroto, A. S. *et al.* Controlled release of nitrogen using urea-melamine-starch composites. *J. Clean. Prod.* **217**, 448–455 (2019).
38. Bortoletto-Santos, R. *et al.* Biodegradable oil-based polymeric coatings on urea fertilizer: N release kinetic transformations of urea in soil. *Sci. Agric.* **77**, 1–9 (2020).
39. Tomaszewska, M. & Jarosiewicz, A. Use of polysulfone in controlled-release NPK fertilizer formulations. *J. Agric. Food Chem.* **50**, 4634–4639 (2002).
40. Kilmer, V. J. & Alexander, L. T. Methods of making mechanical analyses of soils. *Soil Sci.* **68**, 15–24 (1949).
41. Embrapa. Documentos 132 Manual de Métodos de. *Embrapa* 230 (2011).
42. Nelson, D. W. Chapter 34 Total Carbon, Organic Carbon, and Organic Matter. 53711 (1996).
43. Bremner, J. M. & Douglas, L. A. Inhibition of urease activity in soils. *Soil Biol. Biochem.* **3**, 297–307 (1971).
44. Kempers, A. J. & Zweers, A. Ammonium determination in soil extracts by the salicylate method. *Commun. Soil Sci. Plant Anal.* **17**, 715–723 (1986).

Acknowledgments

This work was supported by FAPESP (São Paulo State Research Foundation, grants #2016/09343-6, #2016/10636-8 and #2018/10104-1), CNPq (Brazilian National Council for Scientific and Technological Development, grant #2014/142348-7), and CAPES (Coordination for the Improvement of Higher Education Personnel, Finance Code 001). The authors thank the Agronano Network (Embrapa Research Network), SISNANO/MCTI, and the National Nanotechnology Laboratory for Agribusiness (LNNA) for providing institutional support and facilities. Caue Ribeiro also acknowledges Alexander von Humboldt Foundation and CAPES by Experienced Research Fellowship (CAPES/Humboldt Agreement – Process 88881.145566/2017- 18) and Return Fellowship.

Author contributions

A.S.G., S.F.V., N.D.J., C.R., and L.H.C.M. designed research; A.S.G. and S.F.V. conducted the experiment; G.G.F.G. performed the statistical analyses; A.S.G., S.F.V., G.G.F.G., N.D.J., and C.R. wrote the paper. All authors reviewed the manuscript.

Funding

Open Access funding enabled and organized by Projekt DEAL.

Declarations

Competing interests

The authors declare no competing interests.

Additional information

Supplementary Information The online version contains supplementary material available at <https://doi.org/10.1038/s41598-021-87112-2>.

Correspondence and requests for materials should be addressed to N.D.J. or C.R.

Reprints and permissions information is available at www.nature.com/reprints.

Publisher's note Springer Nature remains neutral with regard to jurisdictional claims in published maps and institutional affiliations.



Open Access This article is licensed under a Creative Commons Attribution 4.0 International License, which permits use, sharing, adaptation, distribution and reproduction in any medium or format, as long as you give appropriate credit to the original author(s) and the source, provide a link to the Creative Commons licence, and indicate if changes were made. The images or other third party material in this article are included in the article's Creative Commons licence, unless indicated otherwise in a credit line to the material. If material is not included in the article's Creative Commons licence and your intended use is not permitted by statutory regulation or exceeds the permitted use, you will need to obtain permission directly from the copyright holder. To view a copy of this licence, visit <http://creativecommons.org/licenses/by/4.0/>.

© The Author(s) 2021